In: Knight, R. J. and McLean, J. R. (Eds.), Shelf Sands and Sandstones.
Canadian Society of Petroleum Geologists, Memoir II (1986), p. 163-179.

WAVE-DOMINATED SHELVES: A MODEL OF SAND-RIDGE FORMATION BY PROGRESSIVE, INFRAGRAVITY WAVES

B. Boczar-Karakiewicz[1] and J. L. Bona[2]

Abstract

Long-crested sand ridges with successive crest-to-crest distances of hundreds to thousands of metres are known to form on shelves. The stability of these sand bodies suggests that they may be time-averaged responses to the complex hydrodynamics of their environment. Consideration of the large scales involved seems to indicate that locally-generated storm waves are not responsible for these structures. Such disturbances may indeed modify existing bars, but do not appear to contribute essentially to the formation and mean features of sand ridges. On "wave-dominated" shelves, a mechanism that may account for systems of sand ridges is associated with the development of infragravity waves (waves with periods of 0.5 to 5 min).

A description of the formation of bars on shelves by the propagation of infragravity waves is proposed. The hydrodynamics of the surface are modelled by a nonlinear, dispersive, shallow-water theory. The wave-induced flux of sediment is calculated using an associated mass-transport velocity. The bed topography is then described using a continuity equation. Such a theoretical description results in a coupled system of nonlinear partial differential equations. This system may be simplified somewhat by using a modal decomposition of the surface wave. The resulting equations are then approximated numerically in order to make quantitative predictions about field situations.

The model was tested against measurements made *in situ* on the Atlantic coast of the U.S.A. (the Delmarva coastal shelf). The agreement between the predictions and the measurements was sufficiently good to warrant some confidence in the mechanism inherent in the model's derivation. Specifically, the successive crest-to-crest distances, which in the model depend only on the mean bed slope and the incident wave conditions, agree quite well with measured values. The long time scale for formation of fully-developed bars that is a property of the model provides an *a posteriori* indication of the stability of these structures. Moreover, general trends in onshore transport and in slow ridge migration due to shore retreat can also be predicted using this model.

Resumé

Les mesures effectuées sur les nombreux plateaux continentaux montrent la présence de systèmes de rides de sable avec des creux successifs distants de centaines de mètres à plusieurs kilomètres. La stabilité de ces figures sédimentaires suggère que leur formation est liée à un régime moyen de l'environnement en question. Leurs échelles horizontales relativement grandes montrent également que la houle du vent, générée localement, ne peut pas contribuer essentiellement à la formation des rides en constituant uniquement un agent modifiant ces figures sédimentaires.

Sur les plateaux continentaux "dominés par la houle" il est proposé un mécanisme qui explique la formation des rides par la houle infragravitationnelle (de période de 0.5 à 5.0 min). La dynamique d'une telle houle est décrite par la théorie dispersive et non-linéaire en eau peu profonde. Le flux des sédiments transportés par la houle dans une couche au-dessus du fond est estimé par les formules du transport de masse. La topographie du fond meuble résulte ensuite d'une relation de continuité appropriée. Le problème est décrit par un système d'équations aux dérivées partielles non-linéaires. Une simplification essentielle de ce système a été introduite par une décomposition modale de la houle de surface. Les équations finales sont résolues numériquement en fournissant les prévisions quantitatives.

Le modèle décrit a été confronté avec des mesures *in situ* effectuées sur le plateau continental de l'Océan Atlantique d'Amérique du Nord (de Delmarva). Ces mesures sont en accord avec les prévisions théoriques quant au mécanisme et au modèle proposé. En particulier, les distances consécutives des creux des rides ne dépendent uniquement que de la pente moyenne du fond et des paramètres de la houle incidente. Ceci montre une concordance assez bonne avec les valeurs mesurées. Le fait que l'échelle temporelle de la formation d'un système de rides est relativement longue d'après le modèle (par rapport à la période de la houle) démontre *a posteriori* la stabilité des figures sédimentaires en question. De plus, les propriétés générales du transport des sédiments vers la côte et la lente migration des rides suivant le retraite lente de la ligne côtière peuvent être également expliquées par les prévisions du modèle proposé.

Introduction

There is, as yet, no agreement about the factors and processes controlling the genesis of sand-ridge topography on continental margins, despite the fact that they are crucial to an understanding of the Holocene transformation of the shelf surface. This is perhaps not so surprising, considering the variety of competing geophysical mechanisms that may contribute to the formation and maintenance of these large-scale sand bodies.

The present paper proposes an explanation of sand-ridge formation by infragravity waves (waves with periods of 0.5 to 5 min). This model predicts the formation and dynamics of sand ridges, and also explains some of their morphological and sedimentological features. In the description of the general hydrodynamic environment, only effects induced by progressive waves are considered. Consequently, the results obtained apply only to what we shall call "wave-dominated" shelves, where reflection is weak and where other currents may be neglected. Excluded from considerations are shelves where partial reflection of the waves is important, as might be described by an appropriate extension of the near-coast theories of Lau and Travis (1973) and Mei (1985), and shelves where tidal currents play a dominant role, as considered in the analysis of Huthnance (1982).

[1]INRS-Océanologie, Université du Québec, 310 Avenue des Ursulines, Rimouski, Québec, Canada G5L 3A1.

[2]Department of Mathematics, The University of Chicago, 5734 University Avenue, Chicago, Illinois, 60637, U.S.A. Present address: Department of Mathematics, Pennsylvania State University, 215 McAllister Hall, University Park, Pennsylvania 16802, U.S.A.

Because of these restrictions, model predictions presented in this paper will be compared with *in situ* measurements reported in field studies on the Atlantic shelf of North America, where reflection is probably small and tidal and other currents appear to have little influence on sedimentation processes (cf. Davies, 1964).

Features of sand ridges on the Atlantic shelf that are the basis of the present study are reviewed in Section 2. A discussion of infragravity waves is presented in Section 3, and the model describing wave-bed interactions is introduced in Section 4. A comparison of model predictions with field measurements for systems of sand ridges on the Atlantic shelf is discussed in Section 5, leading to a set of preliminary conclusions which are reported in Section 6.

Sand Ridges on a Wave-Dominated Shelf

The broad, gently sloping surface of the Atlantic shelf of North America is covered by a large variety of bed forms. A dominating feature is linear, long-crested, sand ridges that often form a rhythmical bed topography; a classical example of which is the sand-ridge field covering the Delmarva inner shelf (Swift *et al.*, 1972a; see Fig. 1). In some 200 of these bed forms, ranging geographically from Long Island to Florida, there is a striking morphological regularity, and a rather specific sediment size distribution (Duane *et al.*, 1972). In addition, these ridges appear to have persisted over decades, despite evidence of a considerable shoreward-directed sediment flux.

An idea of the spatial scales involved and some of the typical features in ridge fields may be obtained from the physiographic sketch shown in Figure 1 (False Cape shelf, Swift *et al.*, 1972a) and from the bathymetric study shown in Figure 2 (Ocean City shelf, after Duane *et al.*, 1972). The distance between successive crests in these fields runs from several hundred metres to several kilometres. Notice that the spacing between adjacent crests increases systematically in the offshore direction as shown in the cross-section of the Ocean City ridge field in Figure 3 (after Duane *et al.*, 1972). Although it is not evident from these cross-sections, Figure 4 (from Duane *et al.*, 1972) shows that the crests and troughs in these ridge fields are aligned roughly parallel to the shelf edge, while at the same time generally lying obliquely with respect to the shoreline.

Across a typical shelf platform, the sand-ridge topography shows a systematic change in morphology. The most regular ridges are found in the outer-shelf regions, whereas the inner-shelf area is characterized by more complexity (the appearance of "secondary crests" in nearer-shore zones is seen in Fig. 1). These changes appear to reflect the gradual change in the hydrodynamic regime that generates and maintains this topography (Swift *et al.*, 1972b; Swift and Field, 1981).

A variety of bed forms (sand waves, megaripples, etc.) coexists with the main ridge-and-trough topography. Of special note are the smallest, the megaripples, which appear morphologically identical to the surf-zone ripples formed by ordinary gravity waves, and so might be construed as evidence for the existence of "megawaves".

Regarding the sediment's grain-size distribution, the study of Swift and Field (1981) on the inner shelf of the Maryland sector has shown a relationship between the grain distribution relative to ridge topography. On the seaward side of a ridge, coarser sand is found, whereas finer sediment occupies the shoreward slopes. Thus, we may think of the grain size distribution as being $\pi/2$ out of phase with respect to the ridge topography as suggested in Figure 5.

The ridge topography on the Atlantic shelf appears to be stable over a time scale of years. Storms, for example that of Ash Wednesday, 1962 (cf. Duane *et al.*, 1972), may have a strong impact locally on sediment transport and beach erosion. In this

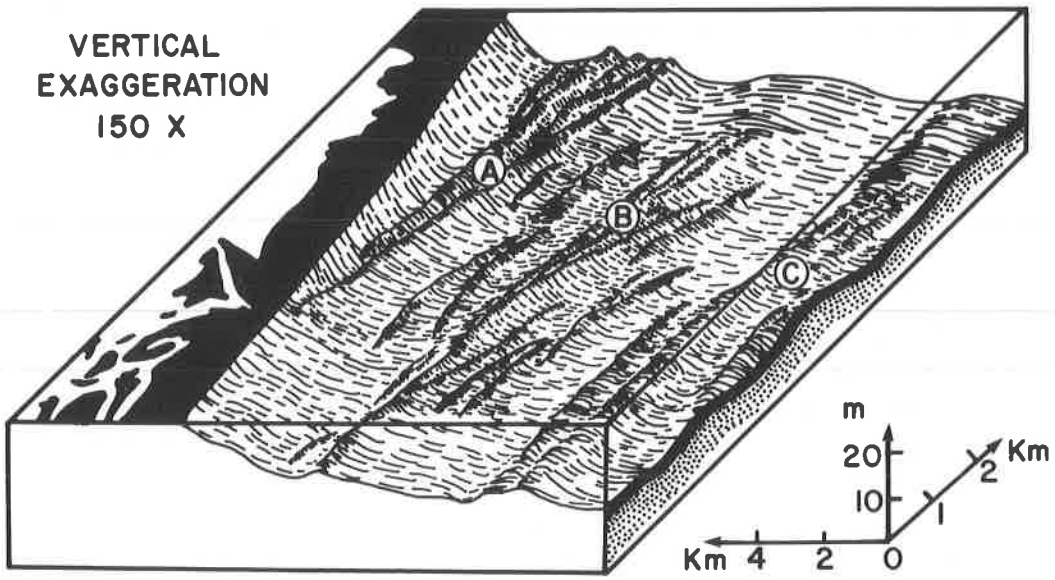

Fig. 1. A classical example of a sand ridge field: a section of the Delmarva inner shelf region (after Swift *et al.*, 1972a).

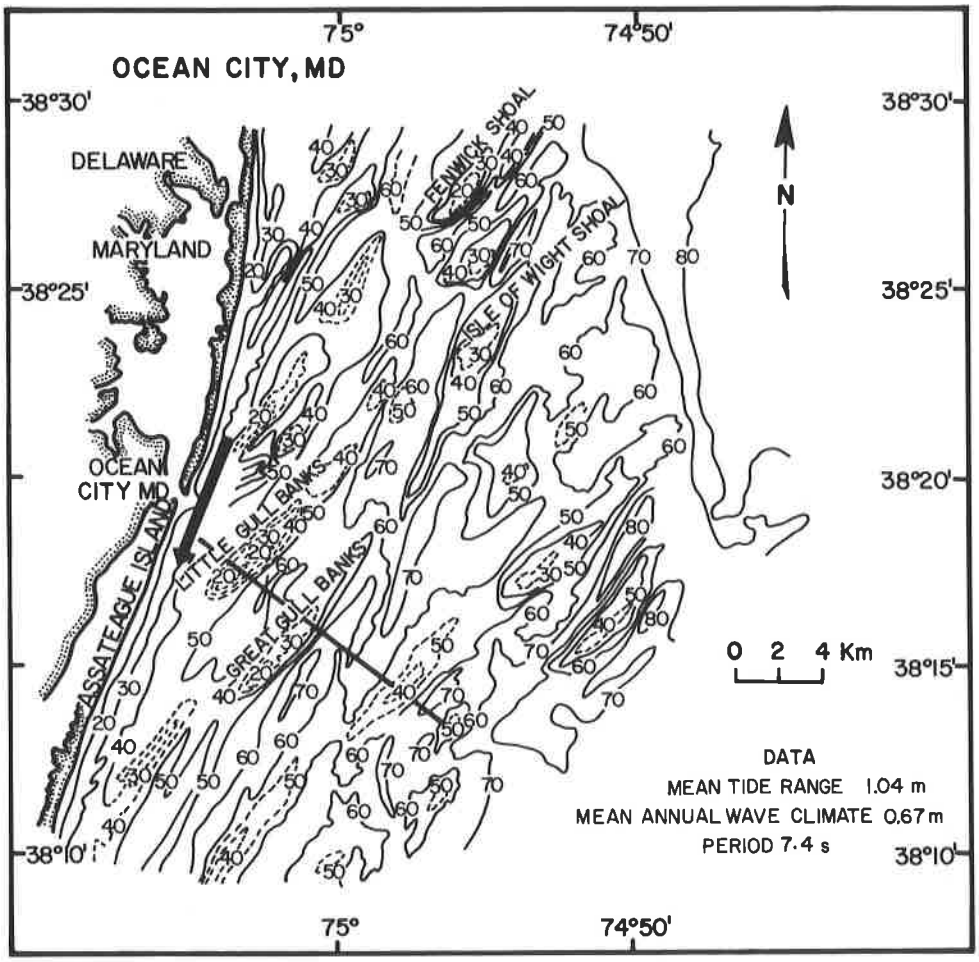

Fig. 2. Location and profiles of a sand ridge field on the Atlantic shelf of North America: Ocean City area (after Duane *et al.*, 1972).

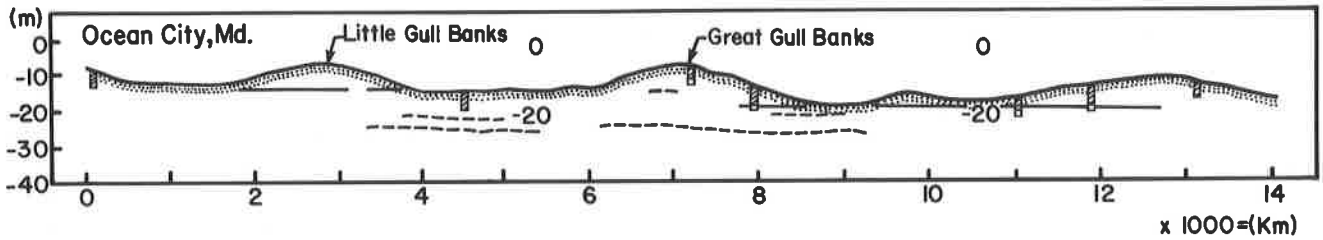

Fig. 3. Cross-section through a sand ridge field on the Atlantic shelf of North America: Ocean City area (after Duane *et al.*, 1972).

example, strong shore-face erosion was nearly compensated for by growth in the sand ridges on the nearby shelf floor, so showing large-scale movement of sediment over quite a short temporal period. However, when the ridge system is viewed as a whole, these short-term changes represent very minor deviations. Thus, one might tentatively conclude that sand ridges are responses more to the average hydrodynamic climate rather than products of intense storms or cyclones, many of which are too localized and moving too rapidly to couple effectively with the water mass lying over the shelf (cf. Vincent *et al.*, 1983).

While major changes are not the rule, over decades impressive departures may occur such as the landward migration of ridges following the slow retreat of the shoreline. Detailed mapping of the Ocean City area shows that the current ridge system has existed in approximately its present location since at least about 1850, with a slight shift of the whole system to the south (Duane *et al.*, 1972). In the False Cape area, a comparison of bathymetric measurements from 1922 to 1969 shows a movement of approximately 350 m of the entire system.

Despite the static nature of these ridge systems, there is nevertheless evidence of a considerable shoreward sediment flux. Pilkey and Field (1972) pursued several lines of inquiry and concluded that beach and estuarine sands on the U.S.A. Atlantic coast are derived in part from the adjacent continental shelf. Even nondeformable substrates appear to be eroded by the vigorous hydrodynamic environment, as heavy minerals

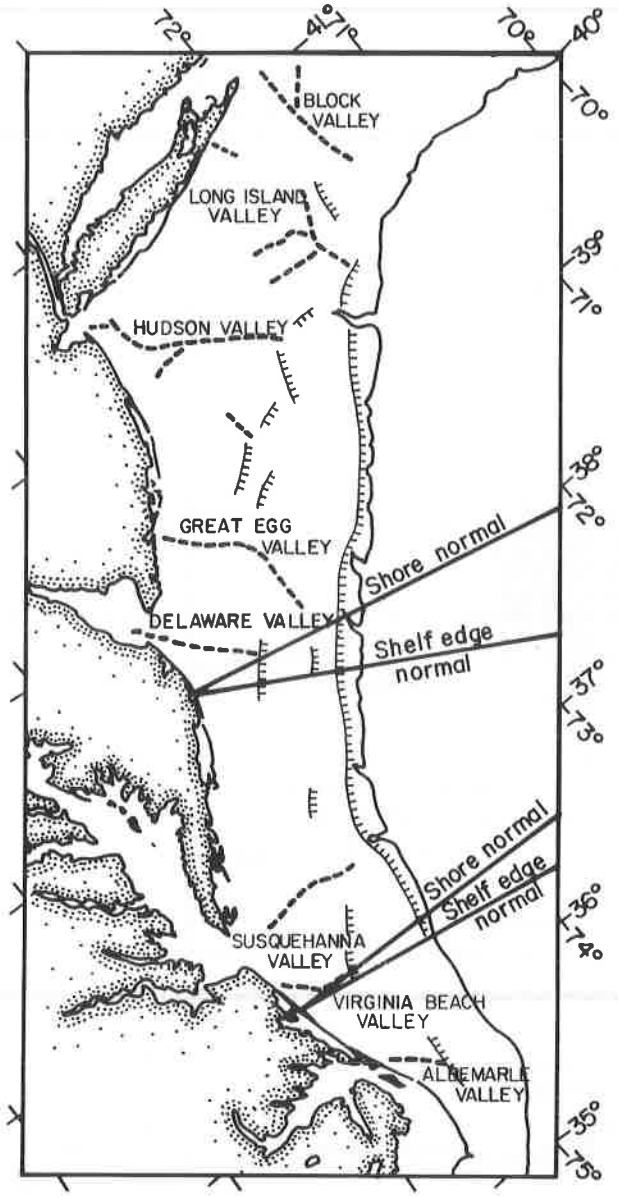

Fig. 4. Shore-normal and shelf-edge-normal orientations for two sand ridge fields (after Swift *et al.*, 1972b).

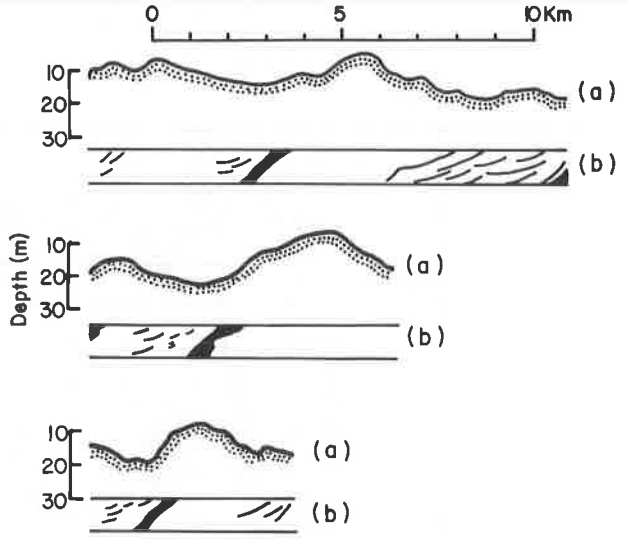

Fig. 5. (a) Profiles of ridge-bathymetries (Maryland coast); (b) side-scan sonar records; coarse sand appears as a black streak, sand wave troughs appear as thinner black lines, (after Swift and Field, 1981).

have been found in the inner-shelf sands and the sands of coastal barriers. The sediment moves at rates in excess of those at which the ridges appear to move, and one is therefore tempted to assume that differential rates of sediment flux are involved in the long-term maintenance of the ridges.

It should be candidly admitted that the points we have described above are not universally accepted. Indeed, perhaps the only point of general accord is that sand ridges are associated with an abundant sediment supply. How the sediment comes to be on the shelf, the role of the sediment supply and the manner of its dispersal on the shelf, and the mechanism leading to the development of stable structures does not appear to be clearly understood. For a wave-dominated shelf, some of these issues will be discussed on the basis of a theoretical model that couples the surface wave regime dynamically with sediment transport and bed deformation.

Infragravity Waves on Shelves

The striking similarity in the external morphology of the linear shoals between Long Island and Florida led Duane *et al.* (1972) to suggest a common genesis for these sand bodies. They also noted that if their origin lay with storm waves or swells, the existence of large-scale sand ridges in water deeper than 12-15 m would simply imply wave heights and periods that are unrealistic for the Atlantic coast. Given that the formation and maintenance of these sand ridges is due to currently active hydrodynamic processes, which seems to be the best hypothesis from all points of view, one must still look outside the range of storm waves and swell to explain the appearance of such structures.

As mentioned in Section 2, the megaripples that are found within the main ridge topography may be formed by the instability of a sandy bed subjected to quasi-periodic gravity waves (cf. Boczar-Karakiewicz *et al.*, 1981, and the references contained therein). Although the formation of such ripples by gravity waves is not fully understood, it should be noted that their local spacing, which is typically a small fraction of the length of the surface waves, is related to the ratio of surface wavelength to depth. If our hypothesis concerning the formation of megaripples on continental shelves is correct, knowledge of the megaripple horizontal scales should allow us to determine the wave periods that generated them. Examples are found on the Oregon shelf (see Komar *et al.*, 1972), where ripples spaced from 10 to 50 cm apart were observed in depths ranging up to 200 m. A simple calculation shows that if the sand ridges are generated in the manner postulated above, then a significant amount of wave energy must reside in periods from 0.5 to 5.0 min.

Such long-period waves, filling the gap in the frequency spectrum between gravity waves and tidal oscillations (Fig. 6), are called infragravity waves. Globally their origin has been loosely linked with wind, very large storm systems, and under-

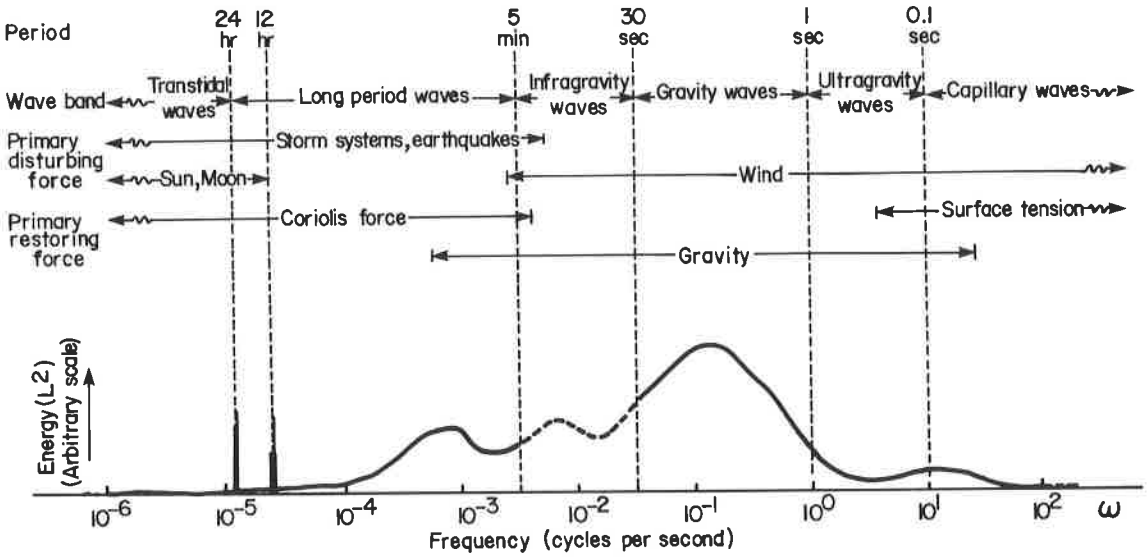

Fig. 6. Schematic representation of the energy contained in the surface waves of the oceans: infragravity wave energy fills the gap between gravity waves and so-called long-period waves (after Kinsman, 1965).

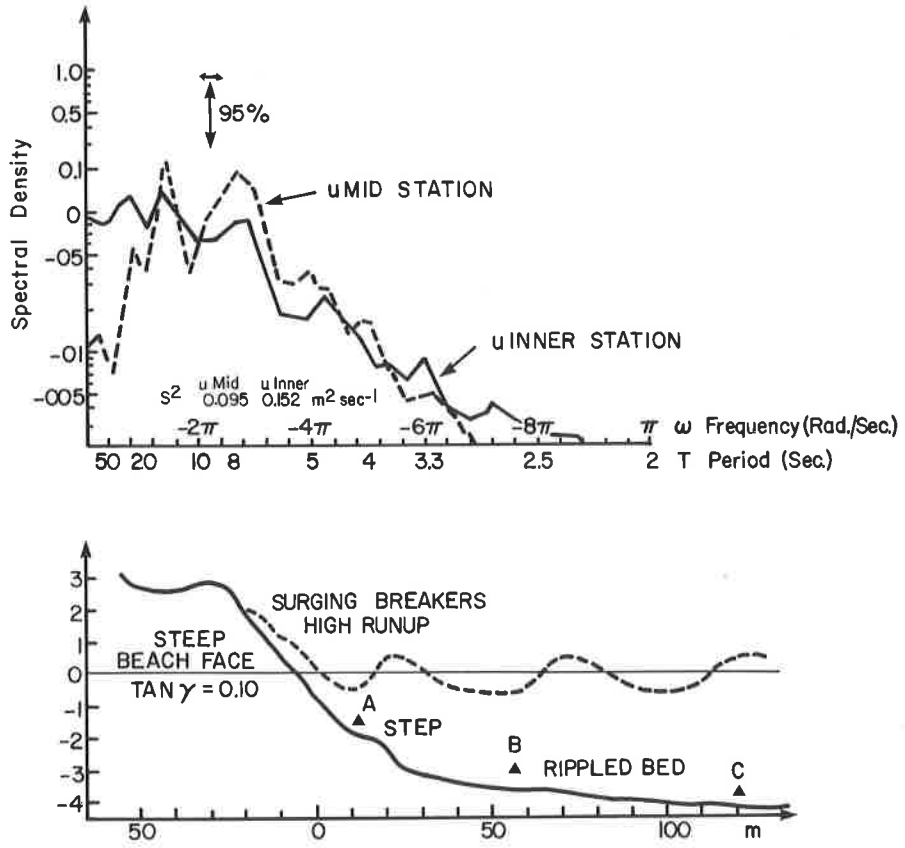

Fig. 7. Typical power spectrum of shore-normal currents on a highly reflective beach (Bracken Beach, Australia; after Wright, 1982).

water seismic activity (Kinsman, 1965). Such waves have attracted attention in various contexts, some of which will be described below, but their possible role in inducing sediment movement on continental shelves has been largely neglected.

Munk (1949) observed large-period (0.5 to 5.0 min) progressive waves impinging upon the nearshore zone. These waves were termed "surf beats", and it was noted that they appeared to be long-crested, and showed no significant longshore variability. Munk and, later, Tucker (1950), attempted an explanation of surf beats in terms of long-period wave groups. The idea was that such groups would have on the whole the same properties, such as breaking and reflection, as a very long-period gravity

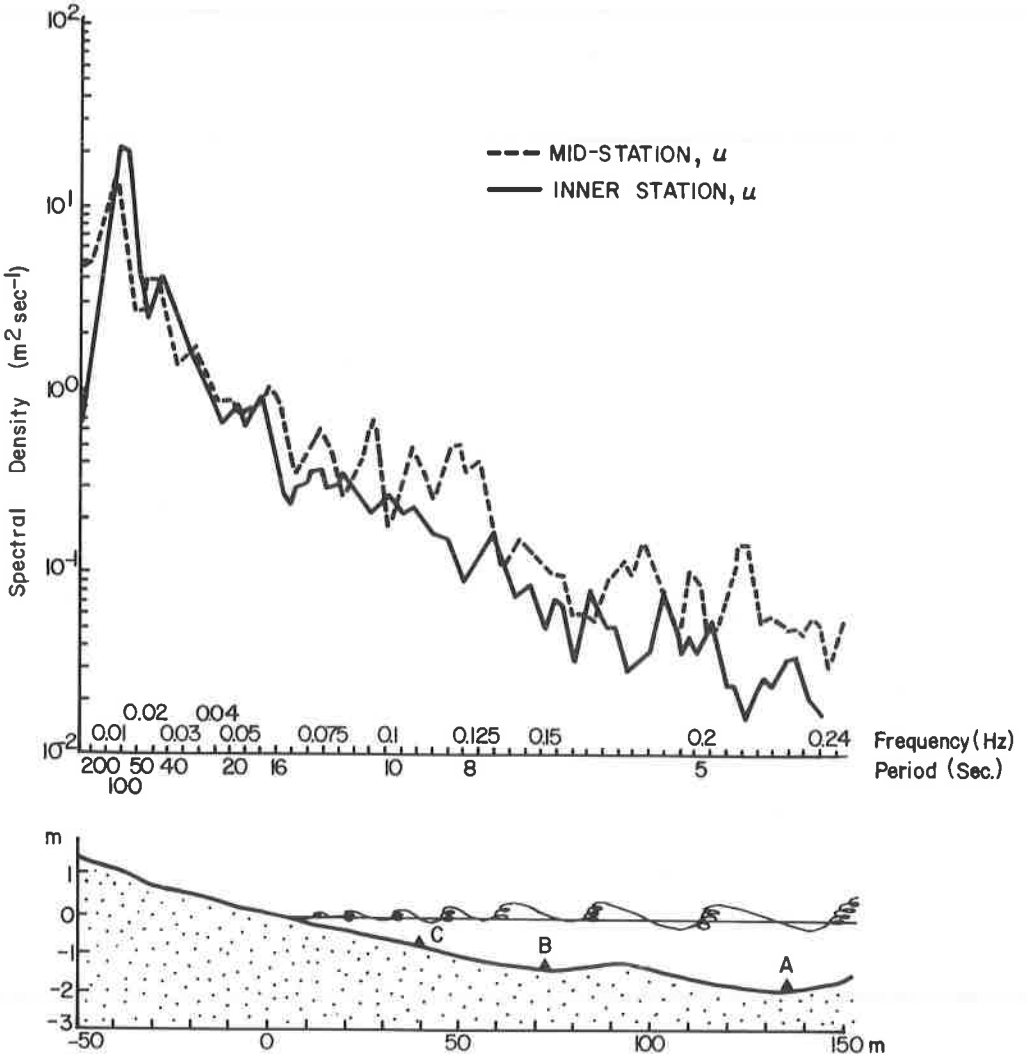

Fig. 8. Typical power spectrum of shore-normal currents on a highly dissipative beach (Goolwa Beach, Australia; after Wright, 1982).

wave. Following this line of thought, Longuet-Higgins and Stewart (1962) put forward the view that the additional momentum flux associated with groups of waves results in the depression of the mean surface. This, it was argued, causes a forced wave to travel to the shoreline, where it is assumed to be reflected as a free wave.

The first systematic field measurements of infragravity waves in the nearshore zone with an associated spectral analysis appears to have been effected by Suhayda (1974) in the Arctic. Several peaks in the energy spectrum were found in the period range from 75 to 120 s. These oscillations were present at the same frequencies in both fair-weather and storm conditions, though the overall energy in the infragravity range increased during storms.

Further evidence of infragravity waves was found near the North Sea coast of Great Britain (Huntley, 1976), and off the coast of Nova Scotia (Holman *et al.*, 1978). Huntley found a group of sharp peaks in the wave-velocity spectrum corresponding to periods in the 20 to 100 s range. During the measurement period off the coast of Nova Scotia, the wave regime varied from calm, through a steady swell, to a fully aroused sea (due to hurricane Bell). Spectral analysis again revealed a sharp peak in the energy spectrum at a period of about 100 s, persisting over the entire range of ambient conditions.

Field studies by Huntley *et al.* (1981) off the California coast focused on wave periods in the 30 to 200 s band. With the swell running at a period of about 14 s, a pronounced energy peak was found at its first subharmonic frequency, and at a frequency corresponding to a 100 s wave period.

Starting with Gallagher (1971), explanations of the sort of observations cited above have been proposed that feature low-frequency, edge-wave oscillations generated in the nearshore zone itself. The contributions of Guza and Davis (1974), Huntley (1976), and Holman and Bowen (1979) are of particular interest in this respect. Some of the measurements already mentioned above showed pronounced longshore variations, indicating that long-period edge waves are an important aspect of nearshore zone infragravity waves. The measurements of Huntley *et al.* (1981) showed onshore-offshore energy levels in the infragravity range to be considerably in excess of that which

which would be expected as radiation on the basis of the edge-wave theories. This led to the presumption of deep-water sources of such waves. The same interpretation was also suggested by Guza and Thornton (1982) in their careful study. Short (1975) was led to presume the existence of obliquely-arriving, long-period, progressive waves as the generating mechanism of linear nearshore bar systems. He established a correlation between the spacing of bars and the wave lengths observed by Suhayda (1974). Thus, despite the validity of theories for the generation of long-period oscillations in the nearshore zone itself, there is still evidence of an offshore origin for such waves.

An extensive study was reported recently (Wright, 1982; Wright *et al.*, 1982) that described measurements taken from a variety of east-coast Australian sites. The observations were made in 7.5 to 11 s, moderate-energy swells on different beaches that included steep reflective, flat dissipative, and intermediate slopes. In all types of topography, oscillations at periods a good deal longer than the swell were detected. The shortest of these seemed to appear on highly reflective beaches (these were identified as zero-mode subharmonic edge waves, Fig. 7). The lowest frequencies, corresponding to periods of 40 to 100 s, were observed in regimes rather like those seen on continental shelves, namely on the flatest, most dissipative beaches (Fig. 8).

Two conclusions for which the foregoing lends some support are important for our model of sand ridge formation. The first is that there are progressive infragravity waves propagating shoreward over the continental shelf. In the absence of conclusive measurements far out on the shelf, we have attempted to infer the existence of such waves from nearshore data. This is somewhat tenuous owing to the more complex infragravity oscillations that are expected in such regions. Nevertheless, the evidence certainly does not exclude our hypothesis. Presuming this conclusion, the next issue of importance for our model concerns the periods of these waves. Here, the situation is perhaps more conclusive. If shoreward-directed infragravity waves are present on a given coastline, then the foregoing evidence points to the period range from 75 to 100 s as typical. We take as a working hypothesis that there is significant energy in incoming progressive waves in these periods.

In the next section these two conclusions will be incorporated into a model for sand-ridge formation.

The Model

In this section, interest is focused on progressive infragravity waves propagating over a sediment-laden shelf. Because of their extreme length, these waves are effectively shallow-water waves which undergo a change of shape in response to the bottom topography. This takes place on a scale corresponding to a few wavelengths. If the bed surface is composed of a movable substance, the passage of the waves may also have an effect on the bottom topography. This latter influence subsists on a much larger time scale, typically of the order of many thousands of wave periods. As the bed deforms, its effect on the incoming waves is consequently modified. Thus, the entire system, comprising both the water and bed surfaces, has the possibility of complex self-interaction.

An idealized version of this system will be considered, and a mathematical model developed to describe it. Suppose that a single-frequency, regular, infragravity wave train with a known constant amplitude propagates shoreward from deep water onto a shelf. Consider further that the waves are long-crested, that they propagate normal to the shelf edge, and that the shelf does not vary appreciably in the longshore direction, so that both the wave and bed motion in question are two-dimensional (see again Fig. 4). Although this idealization is quite restrictive, it is nevertheless known to be approximately valid in laboratory and field situations (Boczar-Karakiewicz *et al.*, 1981; Boczar-Karakiewicz and Bona, 1981). It should be emphasized that we have assumed that infragravity waves are generated outside the shelf, or at least near the edge of the shelf, and that they impinge on the shelf essentially as a sinusoidal wave train. As will be shown presently, incoming infragravity waves more complex than a sine-wave pattern may be accommodated by our model. (In view of the coarse quality of the data with which one must be content in field situations, more complexity may not always be necessary.) However, the presumption that the waves impinge on the shelf from deeper water seems essential to the detailed development of our concept.

The first step in the modelling procedure is to describe the surface-wave motion over relatively short time periods during which the shelf surface may be assumed to be fixed. Consideration of the scales discussed earlier makes it clear that the amplitude $\bar{a}$ may be taken to be small and the wavelength $\bar{L}$ may be taken to be large, compared with the local water depth $\bar{h}$. Thus the Boussinesq equations,

$$\begin{aligned} &q_t + \zeta_x + \alpha q q_x = {}^1\!/_3\, h^2 q_{xxt} + h h_x q_{xt} + {}^1\!/_2\, h h_{xx} q_t, \\ &\zeta_t + [(\alpha\zeta + h)q]_x = 0, \end{aligned} \tag{1}$$

may provide a good approximate description of the wavefield development. Subscripts in (1) denote partial differentiation with respect to the indicated variable. In (1), barred dimensional variables (see Fig. 9) have been nondimensionalized according to the scheme,

$$(h,x,z) = \frac{1}{\bar{H}}\,(\bar{h},\bar{x},\bar{z}), \quad t = (g/\bar{H})^{1/2}\bar{t},$$

$$\zeta = \frac{1}{\alpha\bar{H}}\,\bar{\zeta}, \quad \bar{q} = \frac{1}{\bar{h}+\bar{\zeta}} \int_{-\bar{h}}^{\bar{\zeta}} \bar{u}\, d\bar{z}, \quad q = \frac{\bar{q}}{\alpha(g\bar{H})^{1/2}} \tag{2}$$

where $\bar{H}$ denotes a characteristic depth (e.g., the depth of the water at the shelf edge, g is the magnitude of the acceleration due to gravity, $\alpha = \bar{a}/\bar{H}$, $\bar{x}$ is the horizontal coordinate with $\bar{x} = 0$ at the shelf edge, $\bar{z}$ is the vertical coordinate with $\bar{z} = 0$ at the undisturbed, free water surface, $\bar{u} = \bar{u}(\bar{x},\bar{z},\bar{t})$ is the horizontal component of the velocity field at the point $(\bar{x},\bar{z})$ at time $\bar{t}$, and $\bar{\zeta} = \bar{\zeta}(\bar{x},\bar{t})$ is the deviation of the free surface from its equilibrium position at the point $\bar{x}$ at time $\bar{t}$. Thus q represents a nondimensional, depth-averaged, horizontal velocity.

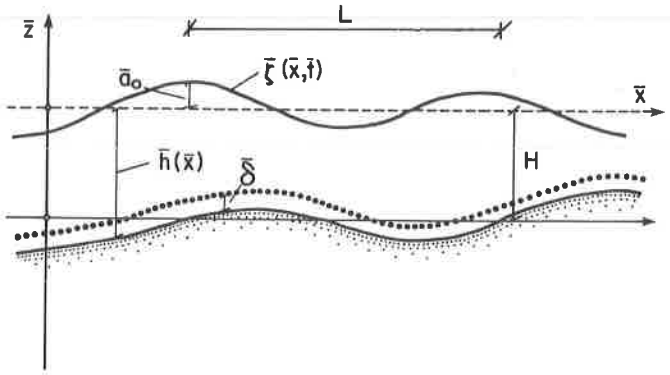

Fig. 9. Definition sketch for the physical variables of the wave field.

Because the initial and boundary conditions needed to render (1) effective exceed the data that one can reasonably expect to obtain in the field, moving on a cruder level of approximation is warranted. Following Lau and Barcilon (1972), the wave amplitude is represented by a simple modal decomposition of the form,

$$\zeta = \zeta(x,X,t) = \sum_{j=1}^{2} a_j(X)\exp(ik_j x - i\omega_j t) + \text{c.c.}, \tag{3}$$

where X is an independent, long, horizontal variable defined by $X = \beta \cdot x$ with $\beta = \bar{H}/\bar{L}$, ω_1 is the frequency of the postulated incoming wavetrain and $\omega_2 = 2\omega_1$ is its second harmonic, k_1 and k_2 are wave numbers associated with ω_1 and ω_2, respectively, by the linearized dispersion relation for equation (1), and the complex, first-order amplitudes a_1 and a_2 are taken to vary on the scale of wavelengths, and therefore are dependent only on the long variable X. In equation (3), and subsequently, c.c. stands for the complex conjugate of the quantity just preceding it, so in this case

$$\text{c.c.} = \sum_{j=1}^{2} a_j^*(X)\exp(iw_j t - ik_j x).$$

A similar representation is postulated for q. (Of course, equation (3) is the truncation of an infinite series. Justification for such a truncation was provided previously in Lau and Barcilon, 1972; Boczar-Karakiewicz *et al.*, 1981; and Boczar-Karakiewicz and Bona, 1981.) Assuming that the principal features of the bottom variation are also gradual, it may also be taken that h is a function $h(X)$ of the long variable X.

When placed in conjunction with the requirements that ζ and q are to satisfy equation (1), the above hypotheses yield the dispersion relation from which k_1 and k_2 are determined, and a coupled pair of ordinary differential equations for the complex amplitudes a_1 and a_2, viz.,

$$\omega_j^2 = \frac{k_j^2}{1 + {}^1/_3\, k_j^2}, \qquad j = 1,2 \tag{4}$$

and

$$\begin{aligned} a_1' &= j_1(X)a_1(X) + \delta_1(X)\, a_1(X)a_2(X)^*, \\ a_2' &= j_2(X)a_2(X) + \delta_2(X)\, a_1^2(X), \end{aligned} \tag{5}$$

where j_1, j_2, δ_1 and δ_2, are functions of X that are determined solely by the wave parameters ω_j and k_j, $j = 1,2$, and the known bottom configuration $h(X)$ (see again Lau and Barcilon, 1972; or Boczar-Karakiewicz and Bona, 1981). The $*$ denotes complex conjugation and the primes in equation 5 denote differentiation with respect to X. The equation 5, when supplemented with the boundary conditions for a_1 and a_2 at $X = 0$, say, provide an approximate description of the evolution of the waveform ζ and the associated depth-averaged velocity q over a given bed configuration h.

We turn now to the impact of the waves on the bed. Taking the bed location to be fixed and known, and assuming a_1 and a_2, and thereby ζ and q, to be determined, it is then straightforward to infer an expression for the tangential fluid velocity at the bed, U_0, from q via the inviscid theory (see Peregrine, 1972). Once U_0 is predicted, there are several ways of attempting to infer an associated sediment movement. One method, which is developed in detail in Boczar-Karakiewicz, Bona and Cohen (*in preparation*), is to take the view that U_0 drives a sediment-laden, laminar, viscous boundary layer which, due to an associated drift velocity, is responsible for a mean transport of sediment mass. The observation that nonlinearity induces a small drift velocity was probably first made by Stokes (1847). It was developed in the context mentioned by Longuet-Higgins (1953) (see also Batchelor (1974, p. 355)). Another possibility would be to take the boundary layer as turbulent (Boczar-Karakiewicz and Chapalain, 1984) or to make use of Bowen's simplification of Bagnold's energy approach to mass transport (see Bagnold, 1963; Bowen, 1980; and Tessier and Boczar-Karakiewicz, 1984). These three ideas do not exhaust the possibilities in this aspect of the modelling (cf. Smith, 1977). However, the general outcome obtained using any of these suggestions is the same (Boczar-Karakiewicz *et al.*, 1985). The results presented in Section 5 were developed from the laminar boundary-layer model. In this case, as for the other models, there is a mass transport velocity $U_m = U_m(X,z,\tau)$, which is a quantity that has been averaged over the fundamental, surface-wave period and so is independent of t, but is assumed to depend on a slow time-variable τ that is appropriate to the description of the bottom deformation. The mass transport velocity leads in turn to a total sediment flux Q_m given by

$$Q_m(X,\tau) = \chi \int_0^\delta U_m(X,z,\tau)\rho(z)dz,$$

where ρ denotes the sediment density in the fluid at height z above the bed, δ is the effective thickness of the boundary layer, and χ is a constant that incorporates various detailed aspects of the sediment. Of course ρ can be taken to be a function of χ and τ as well as of z. The differential movement of the sand is then expressed by the continuity equation

$$\frac{\partial h}{\partial \tau} = -\frac{\partial Q_m}{\partial X}(h,U_0,X). \tag{6}$$

A word concerning the new variable τ is in order here. In all the aforementioned models, the relation between t and τ may be

made explicit using the previously introduced scaling parameters α and β. It turns out that

$$t/\tau \cong \chi \cdot O(\alpha^2\beta^2). \quad (7)$$

In the construction of the turbulent boundary-layer model, the constant χ was shown to be closely related to the sediment concentration in the boundary layer. The value of χ, which has been estimated in laboratory and field situations, appears to be scale-dependent (cf. Boczar-Karakiewicz and Chapalain, 1984; and Boczar-Karakiewicz *et al.* 1985). Extrapolating from laboratory and nearshore values, one would guess that the value of χ relevant to sediment movement on a continental shelf is of the order of 10^{-3} to 10^{-4}. Thus τ/t is of the order of 10^{-9} to 10^{-10}, so providing *a posteriori* justification of the independence of these scales. Note that these rough calculations imply that significant bed movement in response to a changing hydrodynamic environment is to be expected on a time scale of a few months to a few years.

The three coupled equations in (5) and (6) comprise the dynamic description for wave-bottom interaction. To complete the model, auxiliary data must be specified. The underlying spatial domain is $\{X:0 \leqq X \leqq M\}$, with the shelf edge located at $X = 0$, and M chosen appropriately. The depth $\bar{H}$ at the shelf edge is taken as known and is of sufficient magnitude that it is unaffected by the waves, and so remains constant throughout. We assume that an initial bed configuration can be given by $\bar{H}_0(X)$, and that its scaled version can be defined as before by $h_0(X) = \bar{H}_0(X)/\bar{H}$. Thus $h_0(0) = 1$ and the relation $h_0(0,\tau) = 1$ holds for all $\tau \geqq 0$. Also assumed is a fixed, incoming, deep-water, regular wave train with a known amplitude and period. The period of the incoming, infragravity wave train may be estimated from a frequency spectrum and the wave amplitude from the observed energy level in these frequencies (see the discussion in Section 3). From $\bar{H}$, and the amplitude and period of the incoming waves, the parameters α and β are determined, and a scaled mathematical representation of the deep-water wave is defined by

$$A \exp [i(k_1 x - \omega_1 t)] + \text{c.c.}, \quad (8)$$

where the parameter A is complex and order one. A typical choice is to take $A = 0.5$. Other choices of A having the same absolute value simply amount to a change of phase of the incoming wave train. (It should be acknowledged that in field situations the phase of the incoming wave train cannot easily be determined from available data. Thus, there is an inherent error of translation that could be as much as half of the deep-water wavelength. Of course this problem need not arise in laboratory or model basin studies). The incoming, deep-water wave train is accounted for in the model by the boundary conditions on the harmonic amplitudes a_1 and a_2 at the shelf edge $X = 0$. In the case mentioned in equation (8) we take it that

$$a_1(0,\tau) = 0.5; \qquad a_2(0,\tau) = 0.0, \quad (9)$$

for all $\tau \geqq 0$. A more general specification of the incoming wave than that appearing in equation (9) is possible even within the confines of the present model.

A discrete approximation to the dynamic model is outlined below. Notice that the slow temporal variable τ enters only parametrically in the equations in (5), reflecting the assumption that individual waves see the bed as fixed. This feature is used to advantage in the numerical scheme. The instantaneous properties of the wave field at $\tau = 0$ for $X > 0$ are predicted via the equations in (5). These properties depend on the boundary conditions of equation 9. The solution of equation 5 is typically quasi-periodic in space and characterized by a repetition length, L_r, which is usually a few times longer than the fundamental wavelength L of the incoming infragravity wave. This new wave parameter will be discussed in more detail in Section 5. Solutions of the equations in (5) are approximated by a fourth-order, Runge-Kutta scheme, a method that has proven to be efficient, stable, and accurage (Boczar-Karakiewicz, Bona and Cohen, *in preparation*). Once the wave field is determined, a new bed configuration is obtained at time $\tau = \triangle\tau$ by approximately solving equation 6, using a straightforward Euler scheme. With $h = h(X,\triangle\tau)$ in hand, the procedure is reinitiated to obtain a bed profile at $\tau = 2\triangle\tau$, $\tau = 3\triangle\tau$, and so on. In many cases an equilibrium configuration is eventually obtained.

The numerical scheme, briefly described above, turns out to be stable and to converge as the discretization parameters tend to zero. A more detailed account of these ideas are outlined in Boczar-Karakiewicz, Bona and Cohen, (*pers. comm.*). In the next section the proposed model will be tested in the context of continental shelves.

Predictions and Comparisons

In this section we will explore the general characteristics of the solutions of the model presented in Section 4, and make direct comparisons of its predictions with two continental shelf profiles that feature a classical array of sand ridges.

First, for comparison, two sand-ridge fields from the Delmarva shelf are considered, one from the False Cape area (Fig. 1) and one from the Ocean City sector (Fig. 2). The model is initiated without any bed features other than the existing mean slope, estimated from bathymetry to be 0.007 and 0.004 for False Cape and Ocean City, respectively. The incident infragravity wave train is taken to be of moderate amplitude (the parameter α is set at 0.05) with a period of some 80 s (see the extended discussion in Section 2). Such waves are long in comparison to the local depth $h(X)$, over the entire shelf platform, and so may in principle be described using our model.

The outcome of two numerical experiments is presented in Figures 10 and 11. A typical instantaneous wave profile is shown in Figures 10(a) and 11(a). The depiction in Figures 10(b) and 11(b) is the variation of the harmonic amplitudes, $|a_1|$ and $|a_2|$, over the shelf at various times, denoted 0, 1, 2, and 3. In Figures 10(c) and 11(c) the evolution of the initially featureless sloping bed is shown at the same times. Note that the typical wave profiles, the amplitudes of which are enormously exaggerated in comparison to the scale

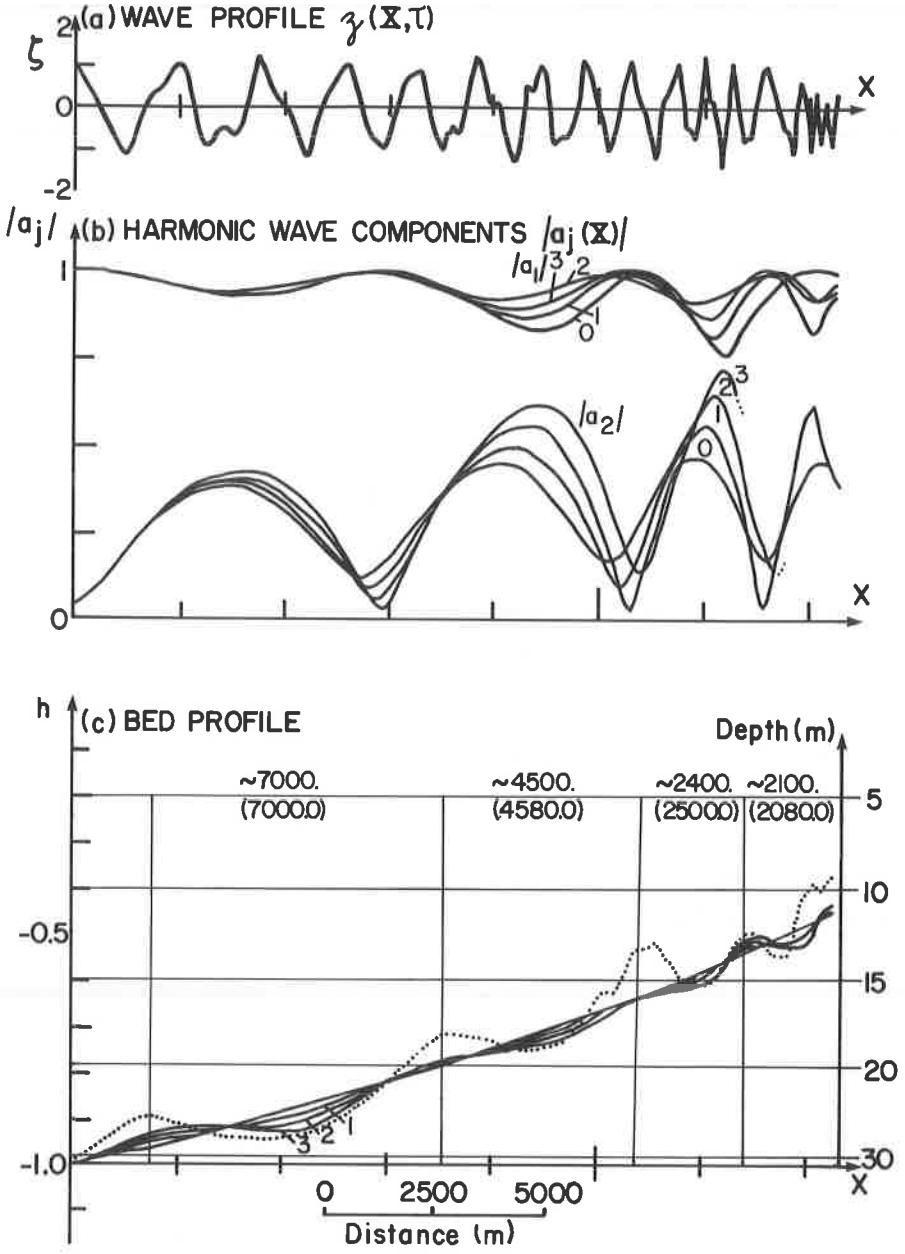

Fig. 10. Prediction of the formation of a sand-ridge system by a long-period surface wave for the False Cape area: (a) final surface-wave profile; (b) evolution of the harmonics of the wave profile; (c) comparison of field measurements (broken line) with predictions of the model (solid line). Note the comparison of the measured crest-to-crest distances (numbers in brackets) with those predicted by the model (numbers without brackets).

of distance from the shelf edge, become progressively more complex as they propagate into shallower water, an effect that coincides with an increase in the relative mean energy in the second harmonic amplitude. It is also clear from Figures 10(b) and 11(b) that this latter effect becomes more pronounced as the bed deforms in response to the wave regime.

Another important aspect of the evolution of the wave field is the strong oscillation of the first and second harmonics that is superposed upon the mean increase in the energy of the second harmonic due to shoaling. As shown in Figures 10(b) and 11(b), energy is exchanged between the wave components in a nearly periodic fashion. The horizontal distance between two successive minima of the second harmonic amplitude $|a_2|$ is referred to as the local *repetition length*, L_r. The repetition length is typically several wavelengths, and it depends on both wave parameters α and β. It decreases with increasing wave amplitude and increases with decreasing wavelength, depending more strongly on β than it does on α (see Boczar-Karakiewicz, Bona and Cohen, *in preparation*). Moreover, L_r appears to decrease with local water depth $h(X)$. The repetition length, L_r, in the wave field induces an associated repetition in the sediment flux term Q_m. The continuity equation, 6, relates the divergence of the sediment flux Q_m with instantaneous, temporal changes in the bed configuration $h(X)$. In such a way the repetition length L_r becomes intimately connected with the spacing of the bars that are observed to form

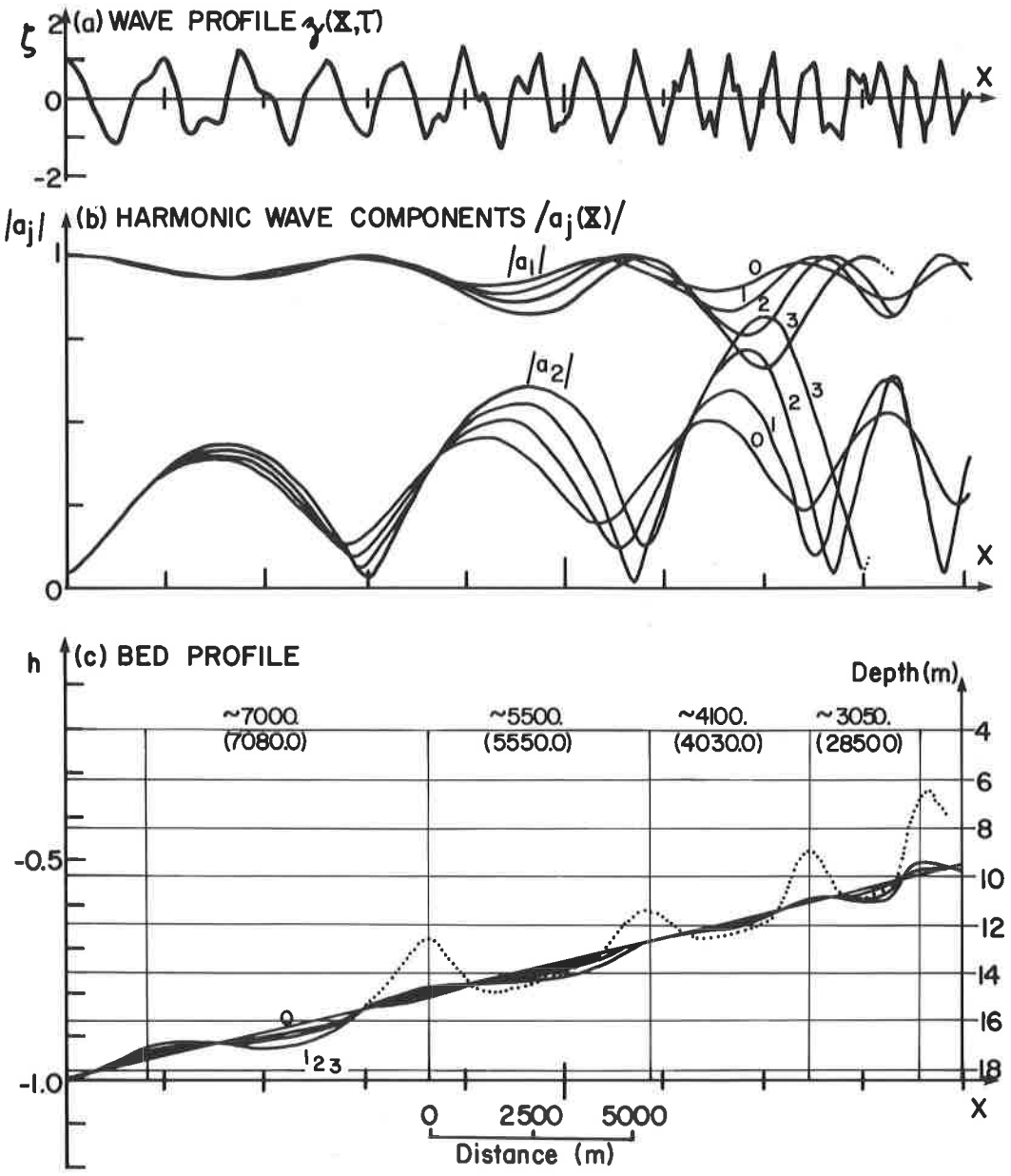

Fig. 11. Prediction of the formation of a sand-ridge system by a long-period surface wave for the Ocean City area: (a) final surface-wave profile; (b) evolution of the harmonics of the wave profile; (c) comparison of field measurements (broken line) with predictions of the model (solid line). Note the comparison of the measured crest-to-crest distances (numbers in brackets) with those predicted by the model (numbers without brackets).

[see Figs. 10(c) and 11(c)]. In parts of the bed configuration where the divergence term $\partial Q/\partial X$ is negative, erosion occurs forming the troughs of the sand ridges; crests are formed where $\partial Q/\partial X$ is positive. Note that for a constant net sediment transport, no changes in bed topography appear. The bed topography reaches a state of equilibrium if, after an initial period of temporal change, the divergence of the sediment flux tends to zero.

The initial, uniformly sloping bed surface develops gradually under the influence of the imposed wave regime into a system of crests and troughs, as shown in Figures 10(c) and 11(c). Although the predicted ridge amplitudes [the full lines in Figs. 10(c) and 11(c)] are not in close agreement with the corresponding field measurements [the broken lines in Figs. 10(c) and 11(c)], the horizontal scales are. A direct numerical comparison of the predicted and observed spacing of ridge crests, shown in Figures 10(c) and 11(c) with the predicted spacing displayed in parentheses under the measured spacing, reveals a relative error in this aspect of only a few percent. Notice that in both cases the horizontal scales in the numerically computed bed form follow the lead of the repetition length L_r in the surface wave. The crest-to-crest scales seem to be slope-dependent with slightly shorter values obtained over the steeper False Cape shelf. With regard to the sand ridge amplitudes, preliminary evidence indicates that better agreement is obtained if dissipation in the wave is taken into account and a more detailed description of the local sediment concentration is introduced into the model of sediment transport in the

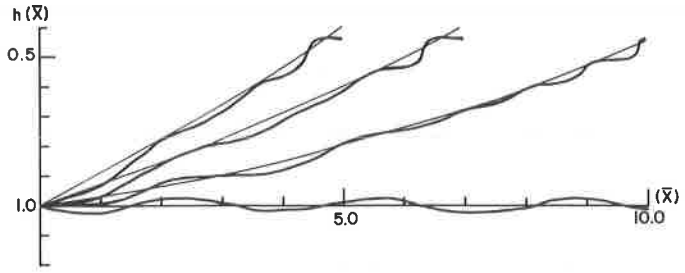

Fig. 12. The model's dependence on the initial mean slope for the wave regime obtained in the Ocean City area.

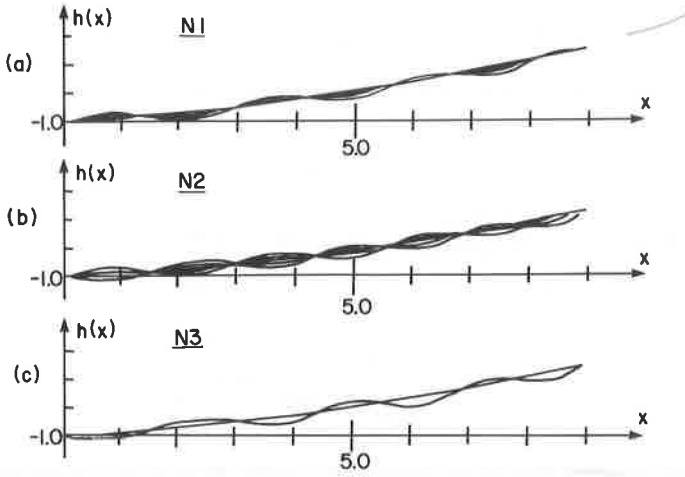

Fig. 13. "Migration" of a sand-ridge system due to an increase in the mean water level: (a) formation of sand ridges for a constant mean water level h_o; (b) rebuilding of the system under an increased water level $h_o + \Delta h$; (c) final landward-shifted system of ridges.

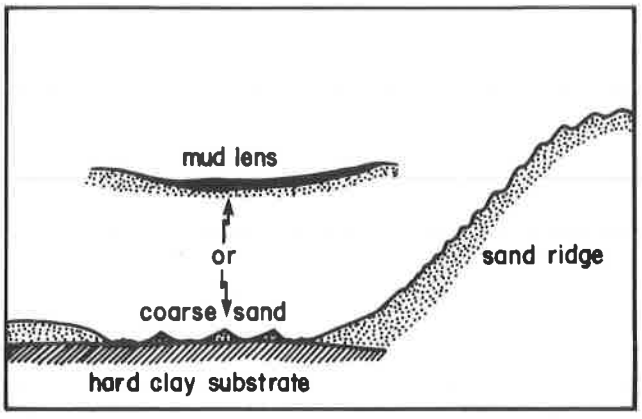

Fig. 14. An example of a typical field situation where the sand ridge crest lies over a nondeformable substrate (after Swift *et al.*, 1972b).

boundary layer. Such improvements are being implemented and will be reported in the future.

Detailed numerical experiments have been carried out to determine how the bar formation is affected by the initial mean slope. A typical result is illustrated in Figure 12, where we see that the number of crests appearing over a given rise in mean bottom level decreases, as does the crest-to-crest spacing, when the mean slope is increased and the other parameters are held fixed. This general trend has been observed many times in the field and laboratory (see the discussion in Section 2).

Slow periodic and nonperiodic changes in the mean sea level were found to have a significant influence on the dynamics of the model, just as they do for actual ridge systems. The results of a numerical experiment simulating a field situation such as that described in Section 2 are shown in Figure 13. A given primary wave is allowed to build a stable ridge system, as in Figure 13(a). The parameters of the model are then changed to reflect an increase in the mean water level, and the numerical integration continued with the previously generated bar system as the initiating bottom configuration. The old system of ridges is rebuilt, as shown in Figure 13(b), to a new, final state displayed in 13(c). Compared with the first ridge system, the new system has migrated landward following a perceived retreat of the shoreline, corresponding to a rise in water level. In contrast, small, periodic, water level oscillations simulating tides do not seem to influence the ridge topography significantly. This was shown by comparing calculations using constant depth parameters and those where water depth was varied periodically by about 10%. A similar bed topography was obtained in both cases.

Another interesting issue concerns the response of a shelf environment with patches of nondeformable substrate, as in Figure 14. On the time scales envisaged, such patches cannot be deformed by hydrodynamic agents. Thus, a unilateral constraint is imposed on the model, that may be enforced by setting the flux Q_m equal to zero at points where the depth reaches the level of the nondeformable substrate. A calculation was performed incorporating this simple device in which an initially featureless sloping bed was taken to be rigid, except for a relatively thin uniform layer of sediment. The result of this calculation is shown in Figure 15(b) and can be compared with the outcome of the same calculation where the entire bed is taken to be deformable, in Figure 15(a). With a rigid substrate, the system develops isolated sediment bodies rather than crests and troughs. A similar outcome was witnessed in a laboratory experiment in which a long-period surface wave propagating over a thin layer of sand with an initial slope of 0.005, formed two isolated sand crests separated by a flat trough, which was the concrete bed of the channel (see Fig. 16).

The present model offers a basis for the observed distribution of sediment sizes on continental shelf ridge systems (see again Fig. 5). As shown in Figure 17, which depicts a numerical experiment starting from a flat, featureless bottom, the ambient boundary layer velocities take on their maximum values on the seaward face of the ridges, while their minimum excursions are recorded on the shoreward faces. The largest

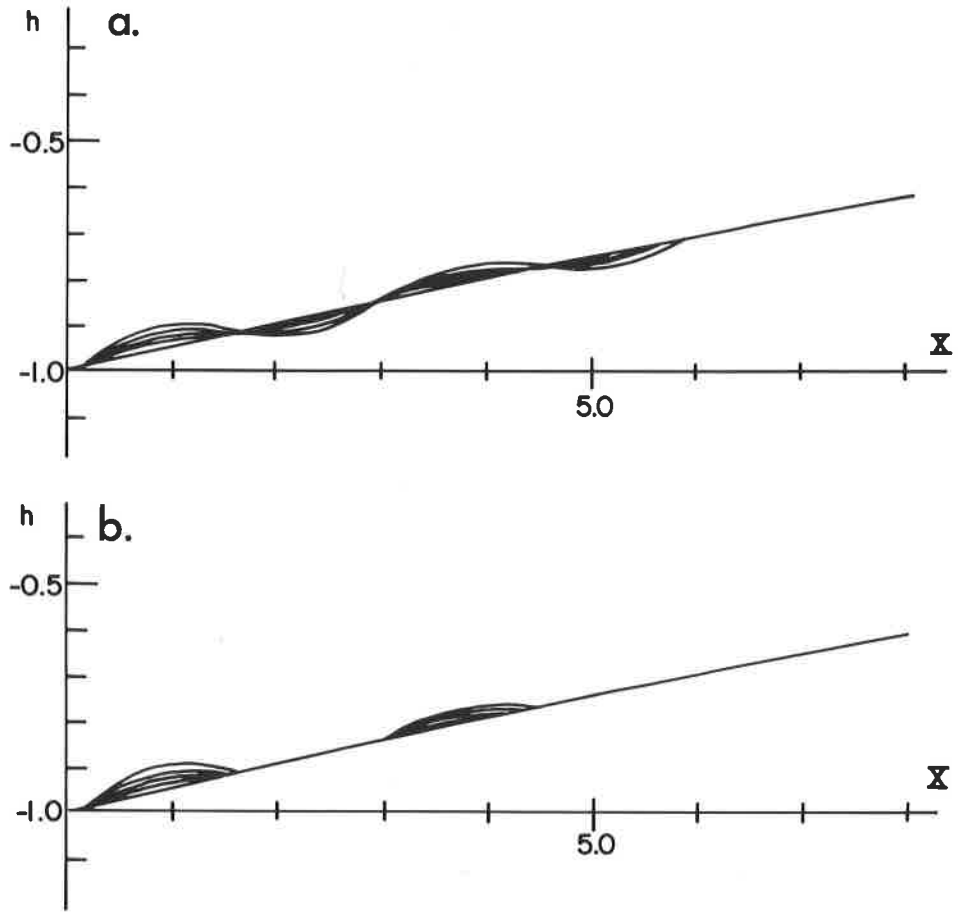

Fig. 15. Formation of sand ridges: (a) over a fully deformable (sandy) bed; (b) over a bed with a nondeformable substrate.

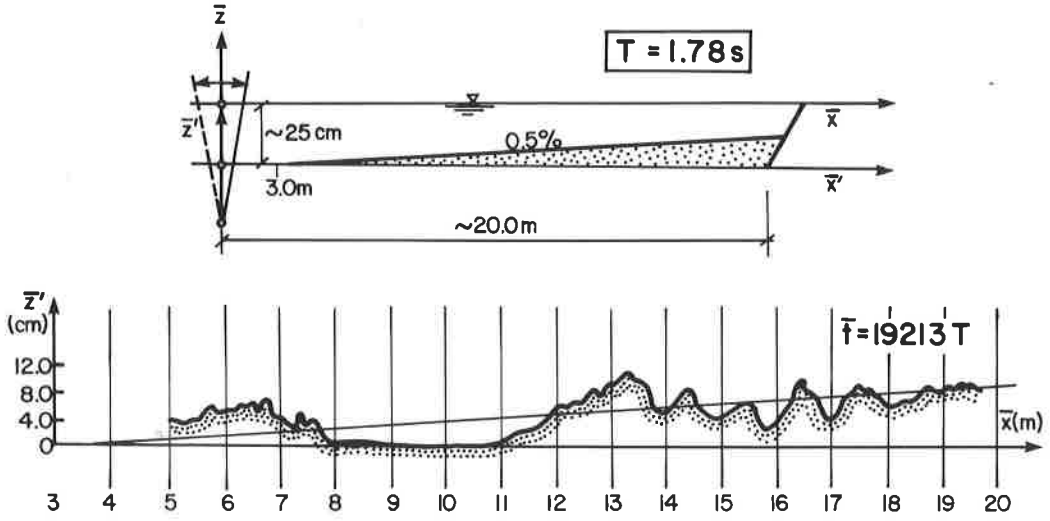

Fig. 16. Formation of sand ridges over a nondeformable substrate. Laboratory experiments (after Boczar-Karakiewicz *et al.*, 1981).

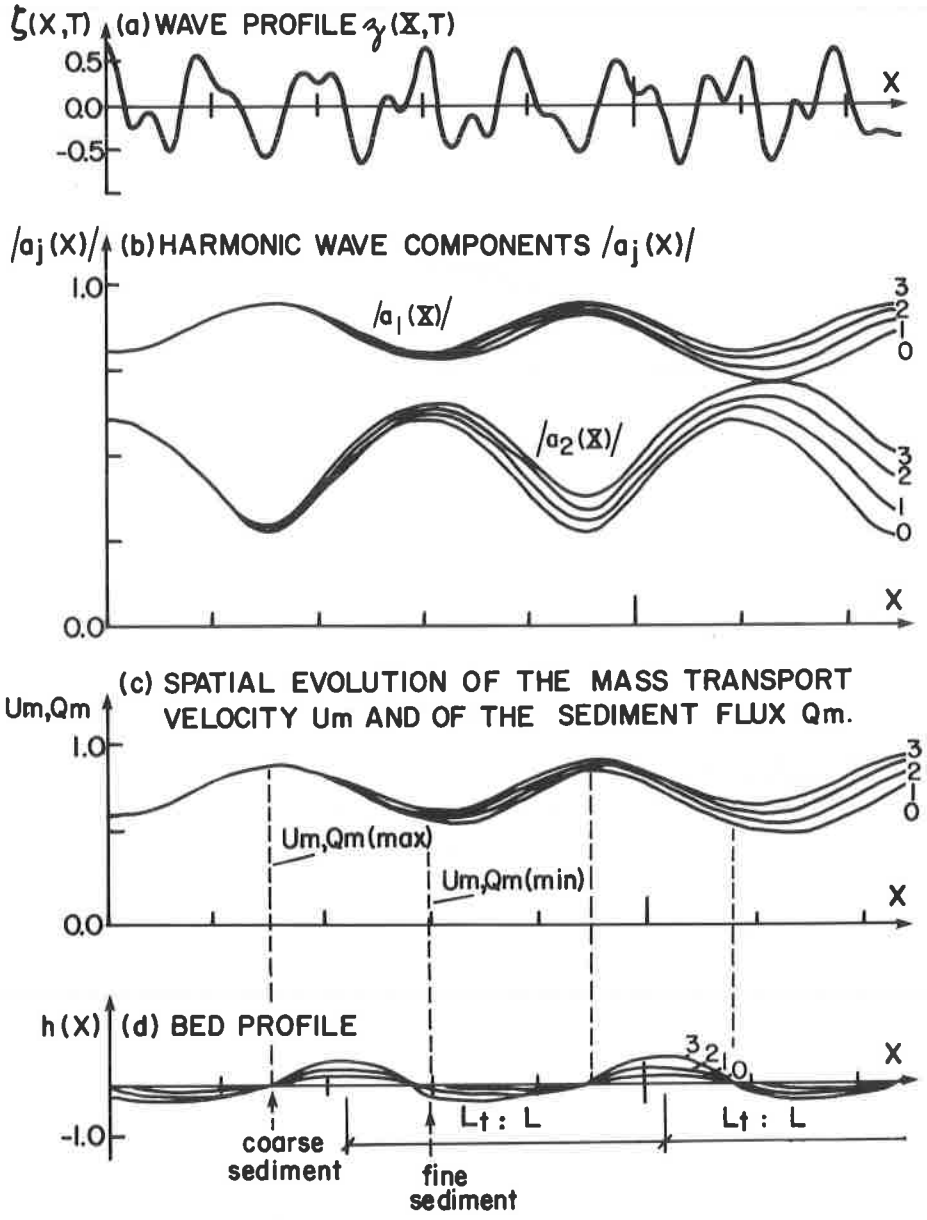

Fig. 17. Relation of wave transformation, sediment transport, and bed deformation for a long-period, progressive, surface wave.

sediment particles capable of responding to the ambient velocities can be moved onto the upper part of the seaward face, but are stationary elsewhere. Hence, a coarser average sediment size will accumulate in this region than elsewhere. This deduction fits the data shown in Figure 5 remarkably well.

Another aspect of the model is that it predicts a continuous, gradual, shoreward-directed flux of sediment. In fact, the mass transport velocity U_m and the sediment flux Q_m are both typically predicted by the model to be everywhere shoreward-directed, while the building and maintenance of the ridges subsists on the differential sediment fluxes. According to Boczar-Karakiewicz, Bona and Cohen (*in preparation*), the model possesses a multi-parameter family of equilibrium configurations which are attractors in the dynamical systems sense, all of which feature a continuous, shoreward movement of sediment. According to the model, the long time scale τ is appropriate for the description of this sediment movement. Insofar as this time scale is short relative to the slow retreat of the shore, the shelf sediment will move toward the shoreline, so giving one possible explanation for the appearance of outer-shelf sands in inner-shelf regions and the sands of coastal barriers. Of course, it should be acknowledged in this context that reflection from the shore was not taken into account in our model. Hence, the conclusions just reached need to be applied with caution in inner-shelf areas, or on shelves with a considerable mean slope.

We also sought to understand the field reports of resonant responses of infragravity waves to particular bed topography. In Figure 18, an example of the results of a sequence of experi-

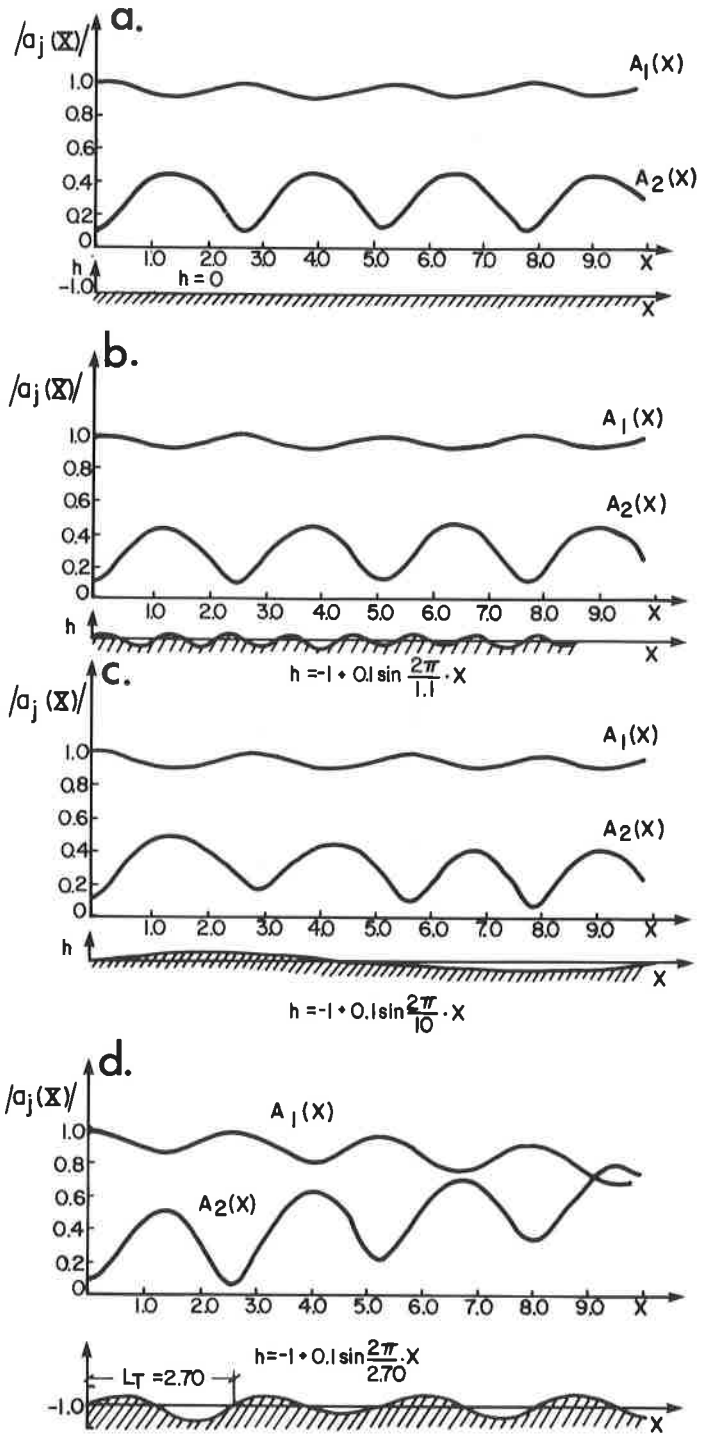

Fig. 18. Effects of bed topography on a long-period, progressive wave: (a) horizontal bed; (b) bed oscillations of shorter horizontal length, and (c) bed oscillations of longer horizontal length than the repetition length, L_r; and (d) bed undulations "tuned" to the horizontal repetition length scale in the wave.

ments using the model are presented. In each of the four cases shown, the incident wave parameters, the constant mean water depth, and the amplitudes of the given bed modulations in cases b, c, and d, were all identical. Figure 18(a) shows a reference calculation over a flat bed; Figure 18(b) shows the same wave over a rapidly modulated bed; Figure 18(c) features a very gradually modulated bottom configuration; and the modulation of the bed in Figure 18(d) is tuned to the repetition length observed over the flat bottom. The surface wave takes little notice of the relatively high frequency and low frequency bed modulations, but this is not the case with its response to the tuned bed in Figure 18(d), where a marked cascade of energy into the second harmonic is evident. Thus, the model indicates that the deformation of periodic long waves propagating in shallow water is not affected significantly by features that recur on a scale very different from the natural repetition length of the waves. Similarly, one would expect infragravity waves on, say, the continental shelf of the eastern United States to interact resonantly with the existing sand ridge fields, though to our knowledge data are lacking to confirm or deny this proposition.

Conclusions

A mechanism is proposed for the formation of large-scale sand ridges by long waves (infragravity waves with a period of the order of 100 s). An example of the comparison between the predictions made using a mathematical model incorporating this mechanism, and field data from the Atlantic shelf of North America is presented in Figure 19. Several general conclusions emerge from the present study that are summarized below.

The correlation between predictions and measurements was quite reasonable, especially if the coarse quality of the initiating parameters is taken into account. In particular, the model predicted:

1. the horizontal distances between adjacent crests in a system of sand ridges would be of the order of kilometres, and would be several times the local wavelength of the incident train.
2. crest-to-crest distances would increase gradually with increasing water depth.
3. crest-to-crest distances and the number of crests would depend on the local mean slope of the shelf platform, both increasing with decreasing slope.

General trends that are observed in the long-term sediment budget and the local sediment size distribution are also explained by the model. These include:

1. The sediment flux due to the action of long-period waves is determined by the mass transport velocity in the bed boundary layer and, in the absence of significant reflection, is always landward directed. However, quantities of sediment displaced by infragravity waves can only be detected by measurements made over long time intervals because of the weakness of the instantaneous rates of transport. This contrasts with sediment movement due to local storm events, which, however, are too isolated in space and time and whose duration is too short to account for the overall generation and maintenance of sand ridge fields.
2. The sediment distrubtion is out of phase with the bed topography due to a corresponding phase shift of the horizontal mass transport velocity distribution.

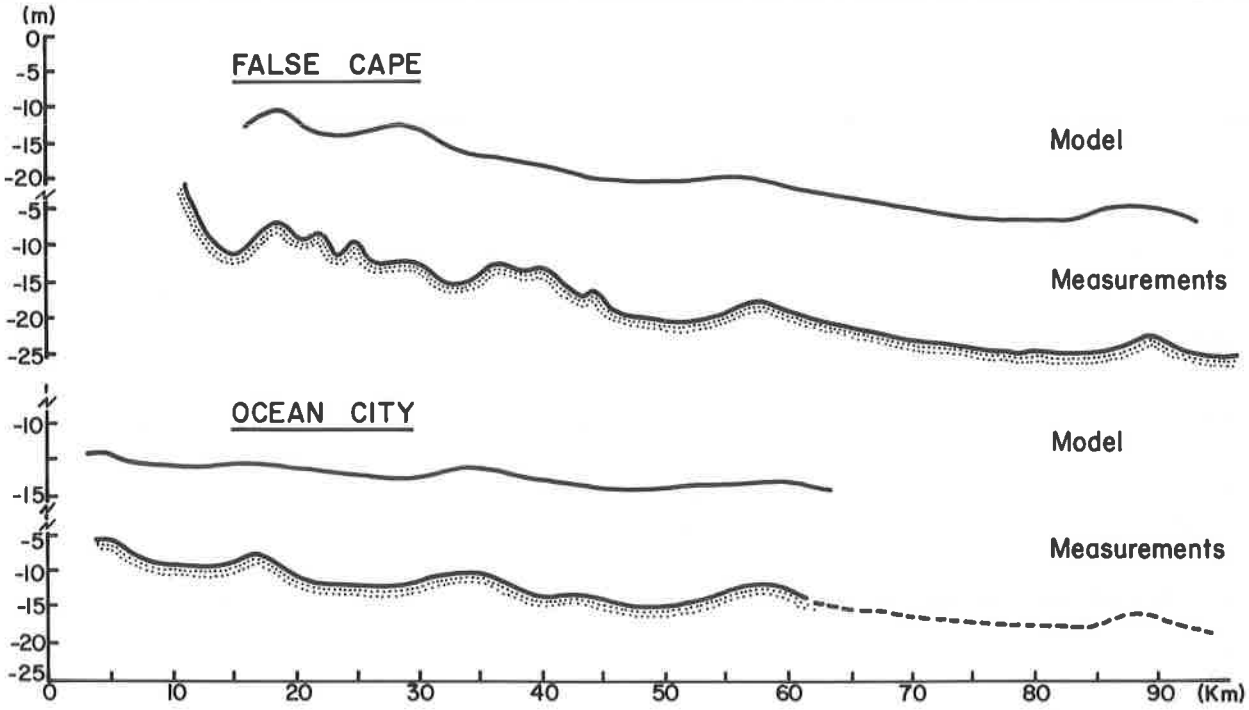

Fig. 19. Model predictions and field measurements for sand ridge fields on the Delmarva shelf.

The dynamics of ridge systems is predicted by the model to have the following features:

1. The migration of ridge systems in the on- or offshore direction is the response of the bed topography to gradual, permanent changes in the mean water level. In contrast, simulated tidal water level changes had little effect on the simulated sand ridges.
2. The formation, maintenance, and stability of sand ridges on a shelf is related to the specific infragravity wave climate, and it is expected that the mutual interaction will produce a resonance phenomenon characterized by a very substantial increase in the mean energy in the second harmonic component.

The reader will readily appreciate that the model proposed herein is at best only a very rough approximation to reality. Nevertheless, the results presented in Section 5 indicate the predictive power of the model with regard to field observations [see also Boczar-Karakiewicz and Bona (1981) and Boczar-Karakiewicz *et al.* (1984)] These results lend credibility to the tentative assertion that, at least in some regimes, the formation of stable, ridge-like structures on continental shelf beds are influenced, perhaps strongly, by the sort of wave/bottom interaction reported in the present study.

References

Bagnold, R. A. 1963. Mechanics of marine sedimentation. *In:* Hill, M. N. (Ed.), The Sea. New York: Interscience, v. 3, p. 507-528.

Batchelor, G. K. 1974. An Introduction to Fluid Dynamics. London: Cambridge University Press.

Boczar-Karakiewicz, B. and Bona, J. L. 1981. Ueber die Riffbildung an sandigen Küsten durch progressive Wellen. Mitteilungen des Leichweiss-Instituts für Wasserbau der Technischen Universität Braunschweig, v. 70, p. 377-420.

——, —— and Chapalain, G. 1985. On sediment transport rates and related time scales for sand bar formation in coastal zones. In: Proceedings of the Canadian Coastal Conference 1985. Forbes, D. L. (Ed.), National Research Council, Ottawa, Canada. p. 271-285.

—— and Chapalain, G. 1984. Sedimentation and bed deformation due to long-wave interactions with a movable bed: turbulent boundary layer model. Internal Report, Institut National de la Recherche Scientifique, Rimouski, Québec, Canada.

——, Drapeau, G. and Long, B. 1984. Modèlisation des barres sableuses littorales de la partie nord des Îles-de-la-Madeleine. Sciences et Techniques de l'Eau, v. 17, p. 35-39.

——, Paplinska, B. and Winiecki, J. 1981. Formation of sand bars by surface waves in shallow water. Laboratory experiments. Rozprawy Hydrotechniczne, v. 43, p. 111-125.

Bowen, A. J. 1980. Simple models of nearshore sedimentation; beach profiles and longshore bars. In: The Coastline of Canada. McCann, S. B. (Ed.), Geological Survey of Canada, Paper 80-10, p. 1-11.

Davies, J. J. 1964. A morphogenic approach to world shorelines. Zeitschrift für Geomorphologie, v. 8, p. 127-142.

Duane, D. B., Field, M. E., Meisburger, E. P., Swift, D. J. P. and Williams, S. J. 1972. Linear shoals on the Atlantic inner continental shelf, Florida to Long Island. *In:* Shelf Sediment Transport: Process and Pattern. Swift, D. J. P., Duane, D. B. and Pilkey, O. H. (Eds.), Stroudsburg, Pennsylvania: Dowden, Hutchinson and Ross, Inc., Ch. 22, p. 447-498.

Gallagher, B. 1971. Generation of surf beat by non-linear wave interactions. Journal of Fluid Mechanics, v. 49(1), p. 1-20.

Guza, R. T. and Davies, R. E. 1974. Excitation of edge waves by waves incident on a beach. Journal of Geophysical Research, v. 79, p. 1285-1291.

—— and Thornton, E. B. 1982. Swash oscillations on a natural beach. Journal of Geophysical Research, v. 87, p. 483-491.

Holman, R. A. and Bowen, A. J. 1979. Edge waves on complex beach profiles. Journal of Geophysical Research, v. 84, p. 6339-6346.

——, Huntley, D. A. and Bowen, A. J. 1978. Infragravity waves in storm conditions. Proceedings of the 16th Conference on Coastal Engineering. New York: American Society of Civil Engineers, Ch. 23, p. 268-284.

Huntley, D. A. 1976. Long-period waves on a natural beach. Journal of Geophysical Research, v. 81, p. 6441-6449.

——, Guza, R. T. and Thornton, E. B. 1981. Field observations of surf beat: 1. Progressive edge waves. Journal of Geophysical Research, v. 86, p. 6451-6466.

Huthnance, J. M. 1982. On one mechanism forming linear sand banks. Estuarine, Coastal and Shelf Science, v. 14, p. 79-99.

Kinsman, B. 1965. Wind Waves: Their Generation and Propagation on the Ocean Surface. Englewood Cliffs, New Jersey: Prentice Hall, Inc.

Komar, P. B., Neudeck, R. H. and Kulm, L. D. 1972. Observations and significance of deep-water oscillatory ripple marks on the Oregon continental shelf. *In:* Shelf Sediment Transport: Process and Pattern. Swift, D. J. P., Duane, D. B. and Pilkey, O. H. (Eds.), Stroudsburg, Pennsylvania: Dowden, Hutchinson and Ross, Inc., Ch. 25, p. 601-620.

Lau, J. and Barcilon, A. 1972. Harmonic generation of shallow water waves over topography. Journal of Physical Oceanography, v. 2, p. 405-410.

——, and Travis, B. 1973. Slowly varying Stokes waves and submarine longshore bars. Journal of Geophysical Research, v. 78, p. 4480-4497.

Longuet-Higgins, M. S. 1953. Mass transport in water waves. Philosophical Transactions of the Royal Society of London, Series A, v. 245, p. 535-581.

——, and Stewart, R. W. 1962. Radiation stress and mass transport in gravity waves, with applications to surf beats. Journal of Fluid Mechanics, v. 13, p. 481-504.

Munk, W. H. 1949. Surf beats. EOS Transactions, American Geophysical Union, v. 30, p. 849-854.

Mei, C. C. 1985. Resonant reflection of surface waves by periodic sand bars. Journal of Fluid Mechanics, v. 152, p. 315-335.

Peregrine, H. D. 1972. Equations for water waves and the approximation behind them. *In:* Waves on beaches and related sediment transport. Meyer, R. E. (Ed.), New York: Academic Press, p. 95-121.

Pilkey, O. H. and Field, M. E. 1972. Onshore transportation of continental shelf sediment: Atlantic southeastern United States. *In:* Shelf Sediment Transport: Process and Pattern. Swift, D. J. P., Duane, D. B. and Pilkey, O. H. (Eds.), Stroudsburg, Pennsylvania: Dowden, Hutchinson, and Ross, Inc., Ch. 21, p. 429-446.

Short, A. D. 1975. Multiple offshore bars and standing waves. Journal of Geophysical Research, v. 80, p. 3838-3840.

Smith, J. Dungan. 1977. Modeling of sediment transport on continental shelves. *In:* The Sea. Goldberg, McCave and O'Brien, (Eds.), New York: Interscience, v. 6, Ch. 13, p. 539-577.

Stokes, G. G. 1847. On the theory of oscillatory waves. Transactions of the Cambridge Philosophical Society, v. 8, p. 441-473.

Suhayda, J. N. 1974. Determining nearshore infragravity wave spectra. International Symposium on Ocean Waves Measurement Analysis, v. 1, p. 54-63.

Swift, D. J. P. and Field, M. E. 1981. Evolution of a classic sand ridge field: Maryland sector, North American inner shelf. Sedimentology, v. 38, p. 461-482.

——, Holliday, B., Avignone, N. and Shideler, G. 1972a. Anatomy of a shore face ridge system, False Cape, Virginia. Marine Geology, v. 12, p. 58-84.

——, Kofoed, J. W., Saulsbury, F. P. and Sears, P. 1972b. Holocene evolution of the shelf surface, central and southern Atlantic shelf of North America. *In:* Shelf Sediment Transport: Process and Pattern. Swift, D. J. P., Duane, D. B. and Pilkey, O. H. (Eds.), Stroudsburg, Pennsylvania: Dowden, Hutchinson and Ross, Inc., Ch. 23, p. 499-574.

Tessier, B. and Boczar-Karakiewicz, B. 1984. On nearshore bars in the Gulf of St. Lawrence: formation, modification and modélisation. Compte rendu du colloque sur la simulation numérique appliquée au domaine de la ressource hydrique. Association Canadienne-Française pour l'Avancement des Sciences (Ed.), 52e Congrès de l'ACFAS, Québec City, Québec, p. 172-186.

Tucker, M. J. 1950. Surf beats: Sea waves of 1 to 5 minute period. Proceedings of the Royal Society of London, Series A, v. 202, p. 565-573.

Vincent, C. E., Young, R. A. and Swift, D. J. P. 1983. Sediment transport on the Long Island shoreface, North American Atlantic shelf: Role of waves and currents in shoreface maintenance. Continental Shelf Research, v. 2, p. 163-181.

Wright, L. D. 1982. Field observations of long-period, surf-zone standing waves in relation to contrasting beach morphologies. Australian Journal of Marine and Freshwater Research, v. 33, p. 181-201.

——, Guza, R. T. and Short, A. D. 1982. Dynamics of a high-energy dissipative surf zone. Marine Geology, v. 45, p. 41-62.